

Sleep Oscillations in the Thalamocortical System Induce Long-Term Neuronal Plasticity

Sylvain Chauvette,^{1,3} Josée Seigneur,^{1,3} and Igor Timofeev^{1,2,*}

¹The Centre de Recherche Institut Universitaire en Santé Mentale de Québec (CRIUSMQ), Laval University, Québec, QC G1J 2G3, Canada

²Department of Psychiatry and Neuroscience, Laval University, Québec, QC G1V 0A6, Canada

³These authors contributed equally to this work

*Correspondence: igor.timofeev@psh.ulaval.ca

<http://dx.doi.org/10.1016/j.neuron.2012.08.034>

SUMMARY

Long-term plasticity contributes to memory formation and sleep plays a critical role in memory consolidation. However, it is unclear whether sleep slow oscillation by itself induces long-term plasticity that contributes to memory retention. Using *in vivo* prethalamic electrical stimulation at 1 Hz, which itself does not induce immediate potentiation of evoked responses, we investigated how the cortical evoked response was modulated by different states of vigilance. We found that somatosensory evoked potentials during wake were enhanced after a slow-wave sleep episode (with or without stimulation during sleep) as compared to a previous wake episode. *In vitro*, we determined that this enhancement has a postsynaptic mechanism that is calcium dependent, requires hyperpolarization periods (slow waves), and requires a coactivation of both AMPA and NMDA receptors. Our results suggest that long-term potentiation occurs during slow-wave sleep, supporting its contribution to memory.

INTRODUCTION

An early study demonstrated that the rate of forgetting is lower during sleep as compared to wakefulness (Jenkins and Dallenbach, 1924). Recent advances propose that a major role of sleep is memory consolidation (Diekelmann and Born, 2010; Maquet, 2001; Siegel, 2005). Both slow-wave sleep (SWS) and rapid eye movement (REM) sleep can contribute to memory consolidation, but early stages of sleep (mainly SWS) increased procedural memory (Gais et al., 2000), and pharmacological blockage of REM sleep did not impair procedural memory (Rasch et al., 2009). Boosting slow oscillation with extracranial fields (Marshall et al., 2006) or training-related increase in slow-wave activity (Huber et al., 2004) correlated with an increased memory retention, suggesting that SWS is critical for memory formation. A plausible physiological mechanism of memory is synaptic plasticity (Bear, 1996; Hebb, 1949; Steriade and Timofeev, 2003). Ocular dominance experiments on young cats demonstrated that sleep plays a crucial role in brain development (Frank

et al., 2001). If indeed SWS induces synaptic plasticity, the signal processing before and after the SWS period should be different; however, physiological data on SWS-dependent modulation of signal processing during the waking that follows sleep are missing.

Intracellular activities of cortical neurons during wake and REM sleep are characterized by steady depolarization and firing, while during SWS the depolarization and firing alternates with hyperpolarization and silence (Chauvette et al., 2010; Steriade et al., 2001; Timofeev et al., 2001). Mimicking neuronal firing during SWS, continuous rhythmic stimulation or repeated trains of cortical stimuli in brain slices were shown to induce steady-state synaptic depression, but synaptic responses were enhanced after the trains of stimuli (Galarreta and Hestrin, 1998, 2000). The repeated grouped firing during SWS resembles the classical long-term potentiation (LTP) protocol (Bliss and Lomo, 1973). Both AMPA and NMDA receptors are subject to long-term plasticity (Kirkwood et al., 1993; Zamanillo et al., 1999) and these receptors are also responsible for sleep-dependent memory formation (Gais et al., 2008). A classical neocortical mechanism of postsynaptic LTP depends on NMDA receptor activation, which leads to calcium entry, and an activation of kinase cascade, including CaMKII, which phosphorylates AMPA receptor and leads to the insertion of GluR1-containing AMPA receptor into synapses (Lisman et al., 2012; Malinow and Malenka, 2002). Increased or reduced activity during wake affected the physiological responses during subsequent sleep (Huber et al., 2006, 2008). Here we used a reversed approach, observing whether sleep will affect responses in the subsequent wake period. We tested the hypothesis that SWS enhances synaptic efficacy via its unique pattern of activities, namely neuronal depolarization and firing (active or up states) intermingled with hyperpolarizing periods (silent or down states), and induces long-term changes in synaptic efficacy.

RESULTS

Evoked Responses Are Potentiated after Slow-Wave Sleep

We recorded multiple electrographic signals from nonanesthetized head-restrained cats, including electro-oculogram (EOG), electromyogram (EMG), and local field potential (LFP) from different cortical areas (Figures 1A–1C). States of vigilance were characterized as in our previous studies (Steriade et al.,

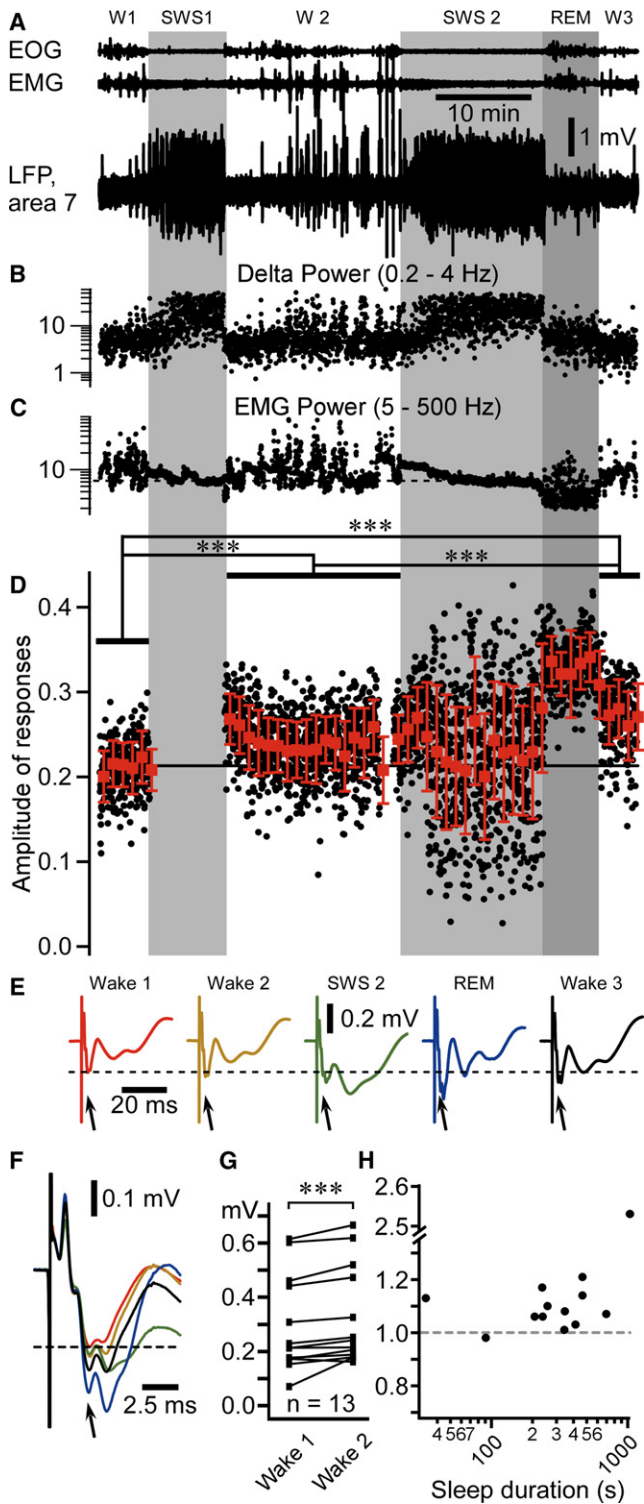


Figure 1. Amplitude of N1 Component of Evoked Potential Responses to Medial Lemniscus Stimuli throughout Sleep-Wake Periods.

(A) Fragment of electro-oculogram (EOG), electromyogram (EMG), and local field potential (LFP) recorded in area 7 of a cat during sleep/wake transitions (W1–W3, Wake; SWS, slow-wave sleep; REM, rapid eye movement sleep.

2001; Timofeev et al., 2001). To study the effect of SWS on synaptic (network) plasticity, we used medial lemniscus stimulation (1 Hz) and recorded the evoked potential responses in the somatosensory cortex during wake/sleep transitions (see [Experimental Procedures](#)). In the example shown in [Figure 1](#), the mean amplitude of the N1 response was $0.213\text{mV} \pm 0.030\text{mV}$ during the first wake episode ([Figures 1D–1F](#)). As the first slow waves appeared in the LFPs, we stopped the stimulation for the whole first episode of SWS and restarted it as soon as the animal woke up (W2); the N1 response was transiently increased and then it was reduced, but it remained enhanced as compared to wake 1; the mean amplitude of N1 response was $0.241\text{mV} \pm 0.037\text{mV}$ during the second wake episode ([Figures 1D–1F](#)). Stimulations were applied in the following sleep episode, which was composed of SWS and REM sleep periods. The responses were highly variable during SWS (SWS2: $0.234\text{mV} \pm 0.073\text{mV}$) and showed the largest amplitude during REM sleep ($0.330\text{mV} \pm 0.035\text{mV}$). The mean amplitude during the third wake episode was further increased (W3: $0.274\text{mV} \pm 0.039\text{mV}$) as compared to the first two wake episodes ([Figures 1D–1F](#)). The amplitude of responses was significantly different in all waking periods ($p < 0.001$ for all comparison, one-way ANOVA, Kruskal-Wallis with Dunn’s multiple comparison test). The SWS-dependent increase in evoked potential did not depend on whether stimulations occurred during SWS (see [Figure S1](#) available online) or not ([Figures 1](#) and [2](#)).

REM Sleep Does Not Play a Significant Role in the Enhancement of Response

On an experimental day, the increase always occurred between the first and the second period of wake and often between the second and the third period of wake. When the increased amplitude of evoked potential saturated after few SWS/wake transitions, the presence of REM sleep did not lead to further enhancement ([Figure 2](#)), as it appears in [Figures 1D–1F](#). In that example, responses were significantly enhanced after the first sleep episode ($0.615\text{mV} \pm 0.144\text{mV}$ in wake 1 versus

Light gray area depicts SWS episodes; darker gray area depicts a REM episode.

(B) Dots represent the delta power (area between 0.2 and 4 Hz in the fast Fourier transform) of 1 s bins from the LFP segment shown in (A).

(C) Dots represent the EMG power.

(D) Black dots represent individual evoked response (N1) amplitude recorded in the LFP of somatosensory cortex (area 3) to the medial lemniscus stimuli (1 Hz). Red squares are the running averages and the error bars represent SD for 60 responses (1 min). *** $p < 0.001$, one-way ANOVA, Kruskal-Wallis with Dunn’s multiple comparison test.

(E) Averaged (area 3) evoked responses for each state of vigilance. The dotted line here and in (F) indicates the voltage of the mean response amplitude in wake 1, and the arrows point to the component of the response that was studied.

(F) Zoom in and superimposition of averages presented in (E) (same color code).

(G) Group data from 13 “wake 1-SWS-wake 2” sequences from four cats. Paired comparison of the mean response amplitude during wake 1 and wake 2 (pre-SWS and post-SWS) episodes is shown. *** $p < 0.001$, Wilcoxon matched-pairs signed-rank test.

(H) Normalized (to wake 1 mean amplitude of evoked response) change in amplitude of response plotted against sleep duration.

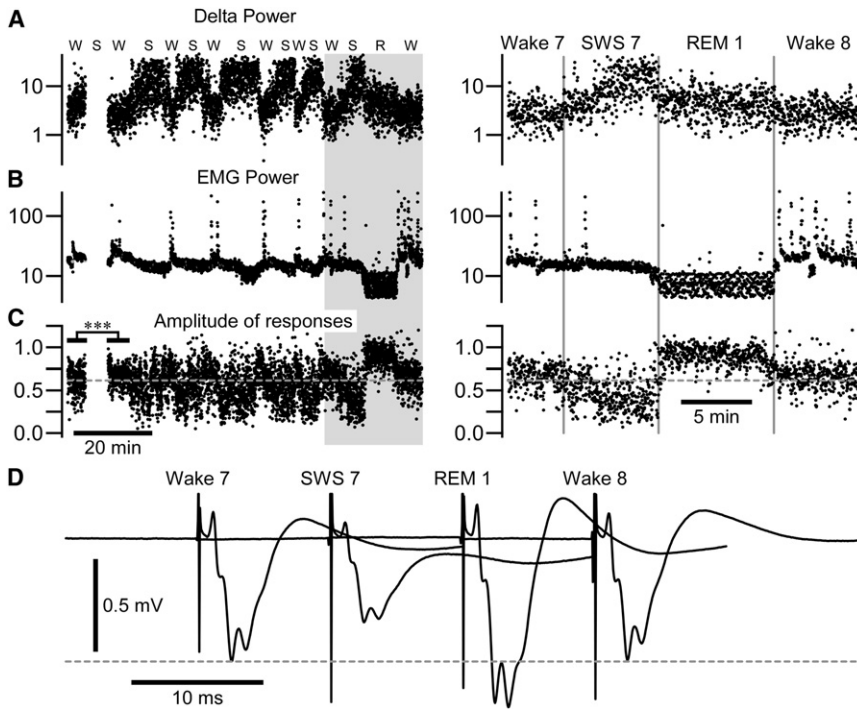


Figure 2. REM Sleep Does Not Potentiate Somatosensory Evoked Potential in a Following Wake Episode

(A and B) The delta power calculated from an area 7 local field potential (A) and EMG power (B) calculated around each medial lemniscal stimulus (± 500 ms).

(C) The amplitude of somatosensory evoked potential. W, wake; S, SWS; R, REM sleep. Note that no stimulation was delivered during the first slow-wave sleep episode and that responses were very significantly enhanced in the second wake episode as compared to the first wake episode; $***p < 0.001$, unpaired t test with Welch's correction. The right panel corresponds to the shaded area in (A), (B), and (C), expanded. The amplitude of response was not enhanced after late REM sleep; $p = 0.7$, unpaired t test with Welch's correction.

(D) Averaged response in each state of vigilance from wake 7 to wake 8, as indicated.

$0.666\text{mV} \pm 0.112\text{mV}$ in wake 2, $p < 0.001$, unpaired t test with Welch's correction) but responses were not further enhanced after the following sleep episodes (no statistical differences in consecutive waking state from wake 2 to wake 8, Figure 2C, $p > 0.05$, one-way ANOVA, Kruskal-Wallis with Dunn's multiple comparison test). However, the response during all waking periods remained significantly different from wake 1 ($p < 0.01$, one-way ANOVA, Dunnett's multiple comparison test). The overall mean amplitude for a first wake episode ($n = 13$, from 4 different cats) was $0.297\text{mV} \pm 0.176\text{mV}$ and it was $0.328\text{mV} \pm 0.177\text{mV}$ during wake 2; this difference was highly significant (Figure 1G, $p < 0.001$, Wilcoxon matched-pairs signed-rank test). Even relatively short periods of SWS were sufficient to enhance responses in the second wake episode (Figure 1H).

Intracellular Responses during Wake-Slow-Wave Sleep-Wake Transitions

We obtained six intracellular recordings from somatosensory cortical neurons in which we recorded evoked responses to medial lemniscus stimuli during two consecutive wake episodes separated by a period of SWS, although it was not always the first and second wake episodes (Figure 3). As expected, membrane potential recordings showed the presence of prolonged silent states during SWS, which were absent during wake (Figure 3A). Responses were highly variable during SWS (data not shown), while they were stable during wake (Figures 3B and 3D). In five out of the six intracellular recordings in which we were able to obtain stable recording throughout wake-SWS-wake transitions (85 recording sessions, near 200 wake-SWS-wake transitions, 2 animals), the response amplitude was increased in the second wake episode (post-SWS) as

compared to the first episode (pre-SWS); however, due to the small number of recordings, the difference was not significant (Figure 3C, $p = 0.2$, Wilcoxon matched-pairs signed-rank test). Therefore, intracellular recordings support field potential observations.

In Vitro, Only the Full Sleep-like Pattern of Stimulation Replicates the In Vivo Results

To characterize the mechanisms implicated in the potentiation of evoked responses, we performed whole-cell recordings from layer II/III pyramidal regular-spiking neurons in vitro. From in vivo LFP recordings, we extracted the timing of a single unit firing recorded during SWS (Figure 4A) and during wake (Figure 5A) and used that timing to build *sleep-like* (Figure 4B) and *wake-like* (Figure 5B) patterns of synaptic stimulation; the timing of slow waves was also detected to build the intracellular hyperpolarizing current pulse stimulation pattern replicating hyperpolarizing (silent) states of SWS (Figure 4B, see Experimental Procedures). The stimulation protocols are detailed in Figure S2. The mean membrane potential of neurons recorded in vitro was maintained to about -65mV to mimic the membrane potential of cortical neurons during wake or active phases of SWS. Minimal intensity stimuli were applied in the vicinity of recorded neurons. The sleep-like pattern of synaptic stimulation induced a transient facilitation only (Figure 4C; $0.640\text{mV} \pm 0.245\text{mV}$ in control versus $0.817\text{mV} \pm 0.144\text{mV}$ in the first minute after conditioning, $p < 0.05$, Mann-Whitney test). A long-lasting facilitation of responses was induced using a combination of sleep-like synaptic stimulation and intracellular hyperpolarizing current pulses with the timing of slow waves (*full sleep-like* pattern, Figure 4D; $0.994\text{mV} \pm 0.527\text{mV}$ in control versus $1.184\text{mV} \pm 0.833\text{mV}$ after conditioning, $p < 0.001$, Mann-Whitney test). The pattern of facilitation was identical to the one observed after a period of SWS (compare Figure 4D with Figure 1D, wake 2), suggesting a similar process leading to this facilitation.

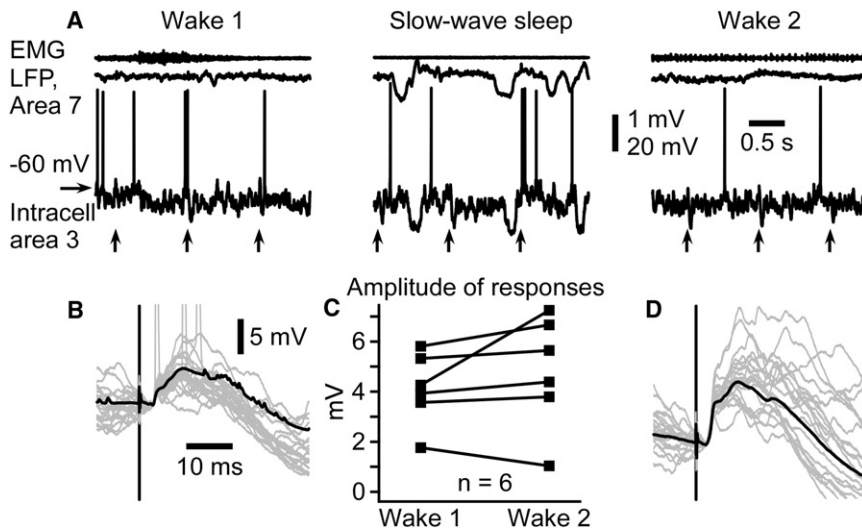


Figure 3. Intracellularly Recorded Evoked Responses Are Enhanced after a Period of Slow-Wave Sleep

(A) EMG from neck muscle, surface LFP from area 7, and intracellular recording from somatosensory cortex in consecutive states of vigilance, as indicated. Vertical arrows indicate the time of medial lemniscus stimulation.

(B and D) Superimposition of 20 individual responses (gray traces) and the averaged response (black trace) during the first (B) and the second (D) episode of wake. Note that responses are ampler in the second episode of wake.

(C) Paired comparison of intracellular response amplitude of six neurons during two consecutive wake episodes separated by a slow-wave sleep episode. Each symbol represents the averaged response amplitude of one neuron during either wake 1 (left) or wake 2 (right). Lines indicate responses of the same neuron in two conditions.

The wake-like synaptic stimulation pattern did not show any facilitation of evoked responses (Figure 5C). To model the neuromodulation activities present during waking state, we added the cholinergic agonist carbachol in the bath (200 μ M), which in agreement with previous observations (Gil et al., 1997) significantly decreased the amplitude of responses in control conditions (Figure 5D; $0.596\text{mV} \pm 0.361\text{mV}$ versus $0.454\text{mV} \pm 0.123\text{mV}$, $p < 0.001$, Mann-Whitney test). After the wake-like synaptic stimulation pattern on the background of carbachol action, we observed only a transient enhancement of responses ($0.679\text{mV} \pm 0.179\text{mV}$, $p < 0.05$, Mann-Whitney test). These results demonstrated that a synaptic activation with the sleep-like pattern of spiking, accompanied with postsynaptic hyperpolarizations (full sleep-like protocol) corresponding to silent states of SWS, was the only tested condition that induced LTP of evoked responses.

Mechanisms of the Enhancement of Responses during the Full Sleep-like Stimulation

Shuffling the timing of synaptic stimulations from the sleep-like pattern, application of intracellular hyperpolarizing current pulses alone, or rhythmic (2.5 Hz) synaptic stimulations did not reveal any long-term plasticity (Figures 6A–6C). The paired-pulse (ISI 50 ms) test showed (1) an enhancement of responses to stimuli after the full sleep-like protocol of stimulation (data not shown), but (2) the paired-pulse ratio did not change (Figure 6D). This combined with the fact that intracellular hyperpolarizing potentials were needed to induce LTP of evoked responses suggests that the enhancement was postsynaptic. Using the full sleep-like protocol of stimulation with BAPTA (25 mM) added to the patch solution to block calcium postsynaptic mechanisms abolished the enhancement of the response (Figure 6E). Adding the NMDA receptor antagonist AP5 (100 μ M) or the AMPA receptor antagonist CNQX (10 μ M) to the bath solution blocked the enhancement of response by either drugs, suggesting that the investigated form of LTP requires a coactivation of both receptor types (Figures 6F and 6G). These results indicate that the mechanism of enhancement

of responses during the full sleep-like stimulation is compatible with the classical LTP.

DISCUSSION

Our *in vivo* results showed that cortical evoked response to medial lemniscal stimuli during wake was enhanced in a subsequent wake episode whether stimuli were applied or not during SWS, supporting the hypothesis of memory consolidation during SWS. Our *in vitro* results showed that only the full sleep-like pattern of stimulation (synaptic + hyperpolarization) mimicking SWS was able to induce the initial transient and the longer-lasting enhancement of responses. Importantly, *in vitro* results showed that this enhancement was postsynaptic, calcium dependent, and required an activation of both NMDA and AMPA receptors matching the classical neocortical postsynaptic LTP.

The cortical slow oscillation has a frequency of about 1 Hz (Steriade et al., 1993). One hertz stimulation usually induces long-term depression in neocortex, but irregular pattern of low-frequency stimulation does not (Perrett et al., 2001). During the silent phase, neurons are hyperpolarized and no firing occurs. During the active phase, neurons are depolarized and multiple presynaptic spikes occur early after the onset of depolarization (Chauvette et al., 2010; Luczak et al., 2007). The network activities during sleep and the experimental protocol of the full sleep-like stimulation used in this study are compatible with protocols of induction of spike-timing-dependent synaptic facilitation (Sjöström et al., 2008). The transition from hyperpolarized to depolarized states coupled with synaptic activities during active states is a natural pattern for spike-timing-dependent plasticity. Therefore, the presence of hyperpolarizing (silent) states appears to be a key component for the induction of LTP during sleep.

According to the sleep synaptic homeostasis hypothesis (Tononi and Cirelli, 2003, 2006), SWS results in a general synaptic downscaling because of a strong reduction in gene expression contributing to LTP (Cirelli et al., 2004; Cirelli and Tononi,

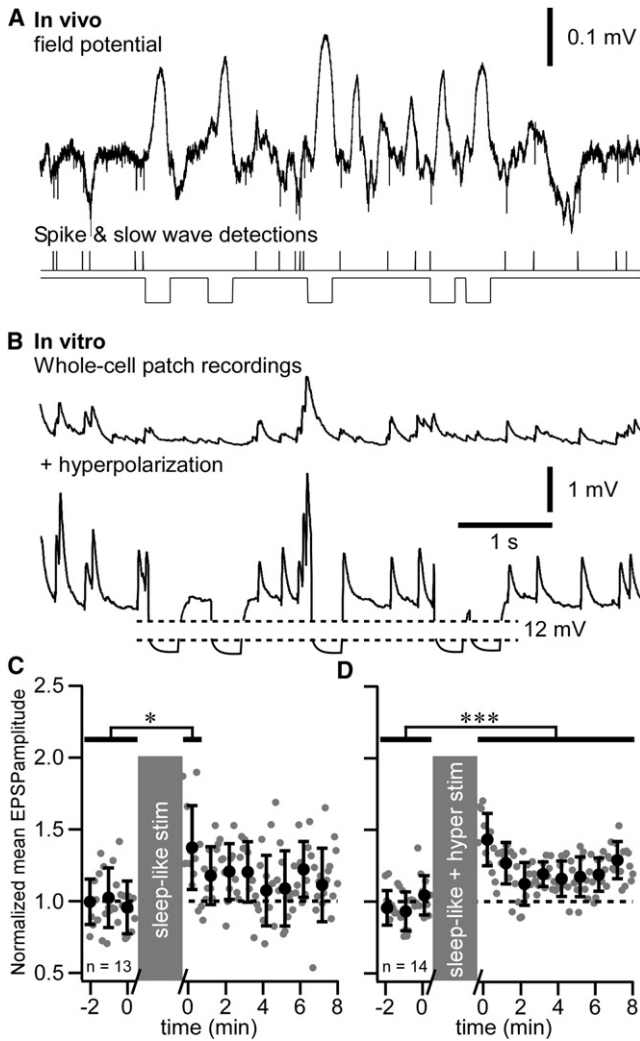


Figure 4. Slow-Wave Sleep Pattern of Synaptic Stimulation Combined to Intracellular Hyperpolarization Pulses Induces Long-Term Potentiation In Vitro

(A) In vivo field potential recording during an SWS period of a cat. Extracellular spikes were detected and their timing was used for the synaptic stimulation pattern. Slow waves were also detected during the same time period and their timing was used for intracellular membrane potential hyperpolarization. (B) In vitro recordings during sleep-like synaptic stimulation pattern (top trace) and during the full sleep-like pattern of stimulation (synaptic + hyperpolarizing pulses, bottom trace). (C) Group data of normalized EPSP amplitude of in vitro whole-cell recordings in control and after sleep-like synaptic pattern of stimulation. (D) Group data of normalized EPSP amplitude in control and after the full sleep-like pattern of stimulation. Gray dots are individual response amplitudes, black circles are the running averages, and error bars represent SD for 12 consecutive responses (1 min). * $p < 0.05$, *** $p < 0.001$, Mann-Whitney test. Grey boxes indicate the 10 min stimulation protocol that was used.

2000a, 2000b). However, the total cortical level of kinase (CaMKII) does not change between sleep and waking state (Guzman-Marín et al., 2006; Vyazovskiy et al., 2008). Other studies have demonstrated that sleep-dependent memory consolidation requires the coactivation of both AMPA and NMDA recep-

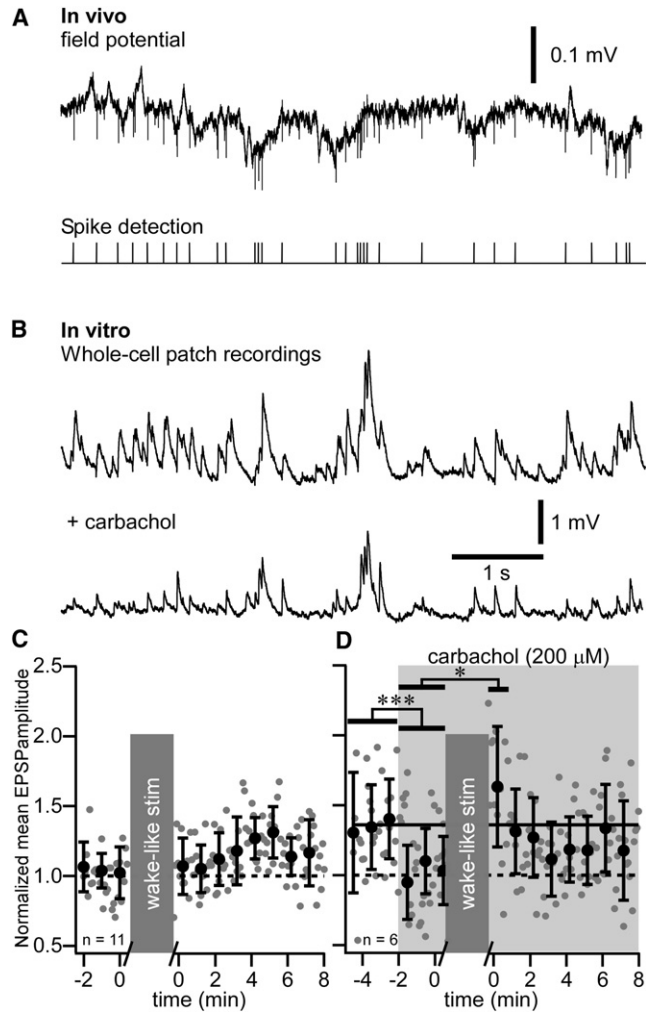


Figure 5. Absence of Long-Term Potentiation after Wake Pattern of Stimulation In Vitro

(A) In vivo field potential recording during waking period of a cat. Extracellular spikes were detected and their timing was used as synaptic stimulation pattern. (B) In vitro recordings during wake-like pattern of synaptic stimulation in control (top trace) and after adding 200 μM of carbachol (bottom trace). (C) Group data of normalized EPSP amplitude of in vitro whole-cell recordings in control and after wake-like pattern of synaptic stimulation. (D) Group data of normalized EPSP amplitude of in vitro whole-cell recordings in control and after wake-like pattern of synaptic stimulation in presence of carbachol (shaded area). Gray dots are individual response amplitudes, black circles are the running averages, and error bars represent SD for 12 consecutive responses (1 min). * $p < 0.05$, *** $p < 0.001$, Mann-Whitney test. Grey boxes indicate the 10 min stimulation protocol that was used.

tors (Gais et al., 2008) and that sleep promotes LTP using a parallel involvement of protein kinase A, CaMKII, and ERK (Aton et al., 2009). Sleep also promotes the translation of mRNAs related to plasticity (Seibt et al., 2012). Classical LTP consists in a calcium entry via NMDA receptors that will activate different kinase cascades, among which CaMKII would play a critical role by phosphorylating AMPA receptor. Once phosphorylated, GluR1-containing AMPA receptors are translocated to the

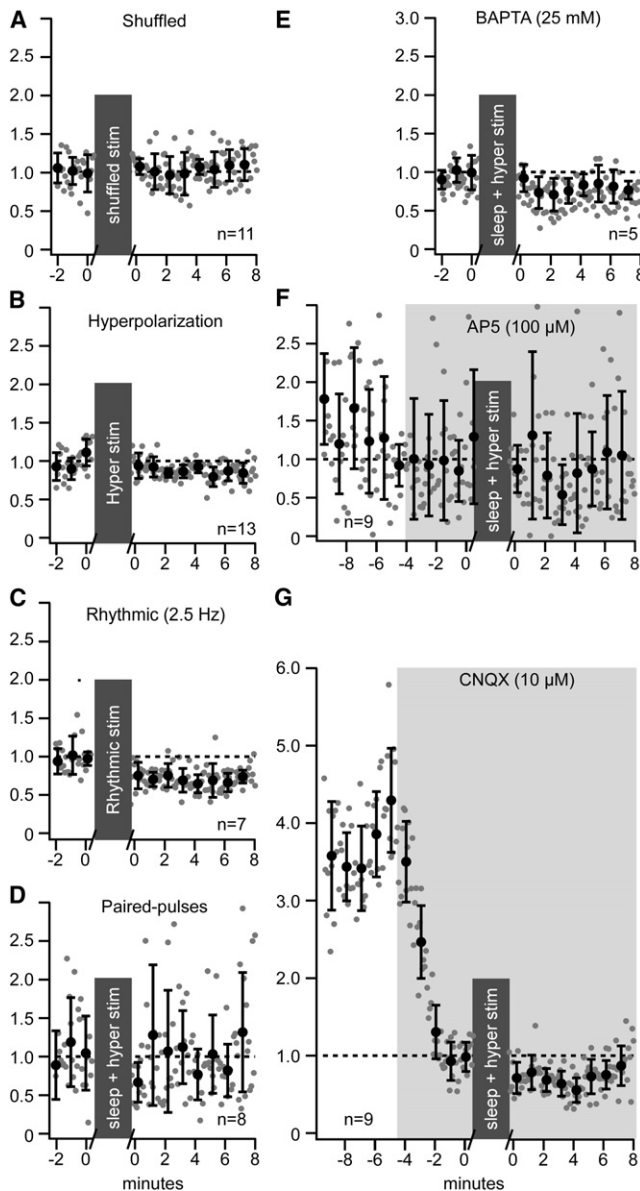


Figure 6. Properties of Long-Term Plasticity Induced by Sleep Pattern of Stimulation

(A) Group data of normalized EPSP amplitude in vitro whole-cell recordings in control and after shuffled timing of sleep pattern of synaptic stimulation. (B) Group data of normalized EPSP amplitude in control and after a period with the hyperpolarization pattern of stimulation only (no synaptic stimulation). (C) Group data of normalized EPSP amplitude in control and after rhythmic pattern of synaptic stimulation (2.5 Hz). (D) Paired-pulse (ISI 50 ms) test applied before and after the full sleep-like stimulation pattern (synaptic + hyperpolarization). (E–G) Group data of normalized EPSP amplitude in control and after period with the full sleep-like stimulation pattern in presence of the calcium chelator BAPTA (25 mM) (E), the NMDA antagonist AP5 (100 μ M) (F), or the AMPA antagonist CNQX (10 μ M) (G). For all panels, gray dots are individual response amplitudes, black circles are the running averages, and error bars represent SD for 12 consecutive responses (1 min). Grey boxes indicate the 10 min stimulation protocol that was used.

synapse leading to LTP. Also, the translocation of AMPA receptors to the synapse (Lisman et al., 2012; Malinow and Malenka, 2002) that probably occurs during SWS does not require new gene expression. This indicates that synaptic potentiation leading to memory formation can occur during SWS despite a reduction in the expression of genes responsible for LTP.

Are there inconsistencies of our results with previous studies? (1) After prolonged waking periods, the slope of callosal evoked responses increases (Vyazovskiy et al., 2008). The earliest phases of evoked potential responses induced by callosal stimulation are composed of antidromic spikes followed by orthodromic spikes (Chang, 1953). This indicates that waking period can increase the excitability of callosal axons. (2) The frequency and amplitude of miniature excitatory postsynaptic currents (mEPSCs) are higher in slices collected from animals after prolonged waking as compared to sleep (Liu et al., 2010). This is likely due to a rebound over excitability in the absence of acetylcholine. Indeed, waking state is characterized by activities of the cholinergic system and acetylcholine reduces the amplitude of excitatory postsynaptic potentials (EPSPs) (Gil et al., 1997; Figure 5D). (3) In somatosensory cortical slices of juvenile rats, calcium-permeable AMPA receptors were shown to be present at the synapse when animals were sacrificed after the wake period and they were absent after the sleep period (Lanté et al., 2011). Obviously, not all types of AMPA receptors are removed from synapses during sleep; thus, it does not preclude the insertion of other AMPA receptor types at synapses during sleep. A recent study in cats showed that intracortical inhibition of mTOR signaling abolished sleep-dependent plasticity, while no effects were observed in the plasticity induced during wake (Seibt et al., 2012). Therefore, it is very likely that plasticity induced during wake or during sleep has different mechanisms.

The stimulation of medial lemniscal fibers is not a learning task per se; thus, it is difficult to affirm whether this experiment simulates a declarative or a nondeclarative learning task. However, most procedural learning tasks implicate the somatosensory system and procedural memory was shown to benefit from SWS (Huber et al., 2004; Rasch et al., 2009), which is also in agreement with our results. The enhancement of responses was always present after the first SWS episode and often also after the second SWS episode, but then the response was saturated. Our results suggest that, once potentiated, the response cannot be further potentiated for a certain time window. This is in agreement with studies on humans showing that mainly early sleep and naps, rich in slow waves, are important for memory improvement (Gais et al., 2000; Mednick et al., 2003; Nishida and Walker, 2007). Our results show a potentiation of cortical responsiveness after a period of SWS and that an imitation of sleep slow oscillation in vitro was sufficient to strengthen the cortical synapses, providing a physiological mechanism for sleep-dependent memory formation.

EXPERIMENTAL PROCEDURES

Experiments were carried out in accordance with the guideline of the Canadian Council on Animal Care and approved by the Laval University Committee on Ethics and Animal Research.

In Vivo Experiments

Experiments were conducted on four adult nonanesthetized cats. The cats were purchased from an established animal breeding supplier. Good health conditions of all animals were certified by the supplier and determined upon arrival to the animal house by physical examination, which was performed by animal facilities technicians and a veterinarian in accordance with requirements of the Canadian Council on Animal Care. The surgery was performed on animals 5–20 days after their arrival to the local animal house. We recorded field potentials and intracellular activities of cortical neurons from somatosensory cortex of cats during natural sleep/wake transitions. We also recorded field potentials from other cortical areas.

Preparation

Chronic experiments were conducted using an approach similar to that previously described (Steriade et al., 2001; Timofeev et al., 2001). For implantation of recording chamber and electrodes, cats were anesthetized with isoflurane (0.75%–2%). Prior to surgery, the animal was given a dose of preanesthetic, which was composed of ketamine (15 mg/kg), buprenorphine (0.01 mg/kg), and acepromazine (0.3 mg/kg). After site shaving and cat intubation for gaseous anesthesia, the site of incision was washed with at least three alternating passages of a 4% chlorhexidine solution and 70% alcohol. Lidocaine (0.5%) and/or marcaine (0.5%) was injected at the site of incision and at all pressure points. During surgery, electrodes for LFP recordings, EMG from neck muscle, and EOG were implanted and fixed with acrylic dental cement. Custom-made recording chambers were fixed over somatosensory cortex for future intracellular recordings. Eight to ten screws were fixed to the cranium. To allow future head-restrained recordings without any pressure point, we covered four bolts in the dental cement that also covered bone-fixed screws, permanently implanted electrodes, and fixed the recording chamber. Throughout the surgery, the body temperature was maintained at 37°C using a water-circulating thermoregulated blanket. Heart beat and oxygen saturation were continuously monitored using a pulse oximeter (Rad-8, MatVet) and the level of anesthesia was adjusted to maintain a heart beat at 110–120 per minute. A lactate ringer solution (10 ml/kg/hr, intravenously [i.v.]) was given during the surgery. After the surgery, cats were given buprenorphine (0.01 mg/kg) or anafen (2 mg/kg) twice a day for 3 days and baytril (5 mg/kg) once a day for 7 days. About a week was allowed for animals to recover from the surgery before the first recording session occurred. Usually, 2–3 days of training were sufficient for cats to remain in head-restrained position for 2–4 hr and display several periods of quiet wakefulness, SWS, and REM sleep. The recordings were performed up to 40 days after the surgery. In this study, the LFP data were analyzed from the first recording session of the day only. Animals were kept awake for at least 1 hr prior to the recording session.

Recordings and In Vivo Stimulation

All in vivo recordings were done in a Faraday chamber. LFPs were recorded using tungsten electrodes (2 M Ω , band-pass filter 0.1 Hz to 10 kHz) and amplified with AM 3000 amplifiers (A-M systems) with custom modifications. We aimed to implant electrodes at 1 mm below the cortical surface. A coaxial electrode (FHC) was implanted in the medial lemniscus fibers for stimulation. Electric stimuli were delivered at 1 Hz in all states of vigilance (wake, SWS, and REM). Given the high spontaneous (\approx 5 Hz) and evoked firing rates (up to 125 Hz) in the cuneatothalamic pathway (medial lemniscus) and the high efficacy of synaptic transmission in this pathway (Alloway et al., 1994), 1 Hz stimulation could not induce synaptic plasticity per se. Intracellular recordings were performed using glass micropipettes filled with 2.5 M potassium acetate and having a resistance of 30–70 M Ω . A high-impedance amplifier with active bridge circuitry (Neurodata IR-283 amplifiers, Cygnus Technology, low-pass filter 10 kHz) was used to record the membrane potential and to inject current into neurons. Intracellular recordings were performed from somatosensory cortex according to the atlas (Reinoso-Suarez, 1961). A silver wire was fixed either in the frontal bone over the sinus cavity or in the occipital bone over the cerebellum and was used as a reference electrode. All electrical signals were digitally sampled at 20 kHz on Vision (Nicolet) and stored for offline analysis. At the end of the experiments, the cats were euthanized with a lethal dose of pentobarbital (100 mg/kg, i.v.).

In Vitro Experiments

Experiments were conducted on 30 Sprague-Dawley rats (postnatal days 21–30, Charles River Laboratories International).

Slice Preparation

Rats were first anesthetized with ketamine-xylazine (40 and 10 mg/kg). The brain was then quickly dissected and maintained in ice-cold artificial cerebrospinal fluid (ACSF) containing the following: 124 mM NaCl, 2.8 mM KCl, 1.2 mM CaCl₂, 2 mM MgSO₄, 1.25 mM NaH₂PO₄, 26 mM NaHCO₃, and 10 mM D-glucose (Sigma-Aldrich Canada) (pH 7.4), aerated with 95% O₂ and 5% CO₂. Osmolarity was 300 \pm 5 mOsm. Coronal slices (350–400 μ m) from one hemisphere were cut with a vibratome to obtain complete sections containing the somatosensory cortex. Slices were transferred to a holding chamber where they were kept at room temperature for at least 1 hr in the same ACSF and aerated with 95% O₂ and 5% CO₂. The brain slices were transferred into a submerged recording chamber maintained at 34°C, containing the perfusion ACSF at a rate of 3 ml/min. The perfusion solution was identical to the cutting solution.

Recordings

Pyramidal neurons in layers II/III were preselected using an infrared differential interference contrast camera microscopy on an upright microscope based on their triangular shape and on their morphology after lucifer yellow 0.2% staining (LY, Sigma Aldrich Canada). We obtained somatic whole-cell current-clamp recordings (10–20 M Ω access resistances) with patch pipettes (resistance between 3–5 M Ω) containing the following: 130 mM potassium D-gluconate, 10 mM 4-(2-hydroxyethyl)-1-piperazineethanesulfonic acid (HEPES), 10 mM KCl, 2 mM MgCl₂, 2 mM ATP, and 2 mM GTP (Sigma-Aldrich Canada) at pH 7.2 and 280 mOsm. In separate experiments, 25 mM BAPTA (Sigma-Aldrich Canada) was added to the patch solution to block calcium. AP5 (100 μ M) or CNQX (10 μ M) (both from Sigma-Aldrich Canada) were also added to the bath solution to block AMPA and NMDA receptors, respectively, and carbachol (200 μ M) (Sigma-Aldrich Canada) was also added to model cholinergic activities during wake. To model wake-like membrane potential values, we injected a steady depolarizing current to maintain the membrane potential near -65 mV.

Cortical Slice Stimulation

Two tungsten electrodes (1–2 M Ω) were placed in layers II/III for extracellular electrical stimulation. Pulses of 0.01–0.02 ms duration and of 0.01–0.15 mA intensity were delivered at a minimal intensity in order to obtain EPSPs and some failures. This intensity of stimulation reproduces the basic properties of single-axon EPSPs in vivo (Crochet et al., 2005). Minimal intensity stimuli were delivered every 5 s in control and after conditioning, because that frequency of microstimulation does not induce synaptic plasticity in cortical slices (Seigneur and Timofeev, 2011).

LFP recordings during natural sleep and waking states were used to extract the timing of a unit firing during wake and during SWS (about 10 min for each state); the timing of onset of slow waves was also extracted from LFP recordings, as described previously (Mukovski et al., 2007). To model silent states in patch-clamp recordings in vitro, we applied hyperpolarizing current pulses of 200 ms (mean silent states during SWS; Chauvette et al., 2011) starting at the exact timing estimated from in vivo LFP recordings. To isolate extracellular spikes, we band-pass filtered the LFP (60 Hz–10 kHz). We used only spikes from single unit recordings. As the unit was well isolated and the spike amplitude was well above the noise level, a threshold was manually set to detect the timing of spikes. An example of such detection can be found in our previous publication (Chauvette et al., 2011). We used the exact timing of spikes detected in vivo to electrically microstimulate cortical slices. Binary files used for stimulation were generated and run in Clampex software (Axon pClamp 9, Molecular Devices) to trigger the stimulators for wake-like, sleep-like, and full sleep-like stimulation pattern applied in vitro (Figure S2). Obviously, no stimuli were delivered during hyperpolarizing states. The sleep-like, full sleep-like, or wake-like stimulation sessions lasted for about 10 min.

To test whether a specific pattern of sleep-like stimuli was needed to induce LTP, we either shuffled the timing of interstimuli intervals using “Randbetween” function from Microsoft Office Excel (shuffled test; Figure 6A) or stimulated them at 2.5 Hz continuously for 10 min to deliver the same number of stimuli as in the sleep-like protocol (rhythmic test; Figure 6C). To test alterations in presynaptic release probability, we used the paired-pulse protocol

(50 ms interstimuli interval) prior and after the full sleep-like stimulation (Figure 6D).

Data Analysis

Electrographic recordings were analyzed offline using custom-written routines in IgorPro software. The delta power was calculated from 1 s sliding time window as the integral power between 0.2 and 4 Hz of full spectrogram; the EMG power was calculated as the integral power between 5 and 500 Hz.

Statistical Analysis

All numerical values are given as mean \pm SD. Specific statistical tests are indicated in the text and in figure legends and were performed in Prism5 (Graphpad software). Briefly, data were first tested for normal distribution and if data had a normal distribution, parametric tests were used; otherwise, the equivalent nonparametric test was used. If only two groups of data were compared, two-tailed unpaired t test with Welch's correction (parametric) or two-tailed Mann-Whitney test (nonparametric) was used. When the data were paired, then two-tailed Wilcoxon matched-pairs signed-rank test (nonparametric) was applied. When more than two groups of data were compared, one-way ANOVA, Kruskal-Wallis (nonparametric) with Dunn's multiple comparison test was applied.

SUPPLEMENTAL INFORMATION

Supplemental Information includes two figures and can be found with this article online at <http://dx.doi.org/10.1016/j.neuron.2012.08.034>.

ACKNOWLEDGMENTS

We thank Sergiu Ftomov for his excellent technical support. This study was supported by grants (MOP-67175 and MOP-37862) from Canadian Institutes of Health Research, Natural Science and Engineering Research Council of Canada (grant 298475), and National Institute of Neurological Disorders and Stroke (1R01NS060870 and 1R01 NS059740). A part of IT salary was covered by Fonds de la Recherche en Santé du Québec via Chercheur National program. S.C. and I.T. performed *in vivo* experiments and the related analysis; J.S. performed *in vitro* experiments and the related analysis. S.C. and J.S. share cofirst authorship. S.C., J.S., and I.T. designed the experiments and contributed to writing the manuscript.

Accepted: August 29, 2012

Published: September 19, 2012

REFERENCES

- Alloway, K.D., Wallace, M.B., and Johnson, M.J. (1994). Cross-correlation analysis of cuneothalamic interactions in the rat somatosensory system: influence of receptive field topography and comparisons with thalamocortical interactions. *J. Neurophysiol.* **72**, 1949–1972.
- Aton, S.J., Seibt, J., Dumoulin, M., Jha, S.K., Steinmetz, N., Coleman, T., Naidoo, N., and Frank, M.G. (2009). Mechanisms of sleep-dependent consolidation of cortical plasticity. *Neuron* **61**, 454–466.
- Bear, M.F. (1996). A synaptic basis for memory storage in the cerebral cortex. *Proc. Natl. Acad. Sci. USA* **93**, 13453–13459.
- Bliss, T.V., and Lomo, T. (1973). Long-lasting potentiation of synaptic transmission in the dentate area of the anaesthetized rabbit following stimulation of the perforant path. *J. Physiol.* **232**, 331–356.
- Chang, H.T. (1953). Cortical response to activity of callosal neurons. *J. Neurophysiol.* **16**, 117–131.
- Chauvette, S., Volgushev, M., and Timofeev, I. (2010). Origin of active states in local neocortical networks during slow sleep oscillation. *Cereb. Cortex* **20**, 2660–2674.
- Chauvette, S., Crochet, S., Volgushev, M., and Timofeev, I. (2011). Properties of slow oscillation during slow-wave sleep and anesthesia in cats. *J. Neurosci.* **31**, 14998–15008.
- Cirelli, C., and Tononi, G. (2000a). Differential expression of plasticity-related genes in waking and sleep and their regulation by the noradrenergic system. *J. Neurosci.* **20**, 9187–9194.
- Cirelli, C., and Tononi, G. (2000b). Gene expression in the brain across the sleep-waking cycle. *Brain Res.* **885**, 303–321.
- Cirelli, C., Gutierrez, C.M., and Tononi, G. (2004). Extensive and divergent effects of sleep and wakefulness on brain gene expression. *Neuron* **41**, 35–43.
- Crochet, S., Chauvette, S., Boucetta, S., and Timofeev, I. (2005). Modulation of synaptic transmission in neocortex by network activities. *Eur. J. Neurosci.* **21**, 1030–1044.
- Diekelmann, S., and Born, J. (2010). The memory function of sleep. *Nat. Rev. Neurosci.* **11**, 114–126.
- Frank, M.G., Issa, N.P., and Stryker, M.P. (2001). Sleep enhances plasticity in the developing visual cortex. *Neuron* **30**, 275–287.
- Gais, S., Plihal, W., Wagner, U., and Born, J. (2000). Early sleep triggers memory for early visual discrimination skills. *Nat. Neurosci.* **3**, 1335–1339.
- Gais, S., Rasch, B., Wagner, U., and Born, J. (2008). Visual-procedural memory consolidation during sleep blocked by glutamatergic receptor antagonists. *J. Neurosci.* **28**, 5513–5518.
- Galarreta, M., and Hestrin, S. (1998). Frequency-dependent synaptic depression and the balance of excitation and inhibition in the neocortex. *Nat. Neurosci.* **1**, 587–594.
- Galarreta, M., and Hestrin, S. (2000). Burst firing induces a rebound of synaptic strength at unitary neocortical synapses. *J. Neurophysiol.* **83**, 621–624.
- Gil, Z., Connors, B.W., and Amitai, Y. (1997). Differential regulation of neocortical synapses by neuromodulators and activity. *Neuron* **19**, 679–686.
- Guzman-Marin, R., Ying, Z., Suntsova, N., Methippara, M., Bashir, T., Szymusiak, R., Gomez-Pinilla, F., and McGinty, D. (2006). Suppression of hippocampal plasticity-related gene expression by sleep deprivation in rats. *J. Physiol.* **575**, 807–819.
- Hebb, D.O. (1949). *Organization of Behavior* (New York: John Wiley & Sons).
- Huber, R., Ghilardi, M.F., Massimini, M., and Tononi, G. (2004). Local sleep and learning. *Nature* **430**, 78–81.
- Huber, R., Ghilardi, M.F., Massimini, M., Ferrarelli, F., Riedner, B.A., Peterson, M.J., and Tononi, G. (2006). Arm immobilization causes cortical plastic changes and locally decreases sleep slow wave activity. *Nat. Neurosci.* **9**, 1169–1176.
- Huber, R., Määttä, S., Esser, S.K., Sarasso, S., Ferrarelli, F., Watson, A., Ferreri, F., Peterson, M.J., and Tononi, G. (2008). Measures of cortical plasticity after transcranial paired associative stimulation predict changes in electroencephalogram slow-wave activity during subsequent sleep. *J. Neurosci.* **28**, 7911–7918.
- Jenkins, J.G., and Dallenbach, K.M. (1924). Obliviscence during Sleep and Waking. *Am. J. Psychol.* **35**, 605–612.
- Kirkwood, A., Dudek, S.M., Gold, J.T., Aizenman, C.D., and Bear, M.F. (1993). Common forms of synaptic plasticity in the hippocampus and neocortex *in vitro*. *Science* **260**, 1518–1521.
- Lanté, F., Toledo-Salas, J.C., Ondrejčák, T., Rowan, M.J., and Ulrich, D. (2011). Removal of synaptic Ca²⁺-permeable AMPA receptors during sleep. *J. Neurosci.* **31**, 3953–3961.
- Lisman, J., Yasuda, R., and Raghavachari, S. (2012). Mechanisms of CaMKII action in long-term potentiation. *Nat. Rev. Neurosci.* **13**, 169–182.
- Liu, Z.-W., Faraguna, U., Cirelli, C., Tononi, G., and Gao, X.-B. (2010). Direct evidence for wake-related increases and sleep-related decreases in synaptic strength in rodent cortex. *J. Neurosci.* **30**, 8671–8675.
- Luczak, A., Barthó, P., Marguet, S.L., Buzsáki, G., and Harris, K.D. (2007). Sequential structure of neocortical spontaneous activity *in vivo*. *Proc. Natl. Acad. Sci. USA* **104**, 347–352.
- Malinow, R., and Malenka, R.C. (2002). AMPA receptor trafficking and synaptic plasticity. *Annu. Rev. Neurosci.* **25**, 103–126.
- Maquet, P. (2001). The role of sleep in learning and memory. *Science* **294**, 1048–1052.

- Marshall, L., Helgadóttir, H., Mölle, M., and Born, J. (2006). Boosting slow oscillations during sleep potentiates memory. *Nature* 444, 610–613.
- Mednick, S., Nakayama, K., and Stickgold, R. (2003). Sleep-dependent learning: a nap is as good as a night. *Nat. Neurosci.* 6, 697–698.
- Mukovski, M., Chauvette, S., Timofeev, I., and Volgushev, M. (2007). Detection of active and silent states in neocortical neurons from the field potential signal during slow-wave sleep. *Cereb. Cortex* 17, 400–414.
- Nishida, M., and Walker, M.P. (2007). Daytime naps, motor memory consolidation and regionally specific sleep spindles. *PLoS ONE* 2, e341.
- Perrett, S.P., Dudek, S.M., Eagleman, D., Montague, P.R., and Friedlander, M.J. (2001). LTD induction in adult visual cortex: role of stimulus timing and inhibition. *J. Neurosci.* 21, 2308–2319.
- Rasch, B., Pommer, J., Diekelmann, S., and Born, J. (2009). Pharmacological REM sleep suppression paradoxically improves rather than impairs skill memory. *Nat. Neurosci.* 12, 396–397.
- Reinoso-Suarez, F. (1961). *Topographischer Hirnatlas der Katze, für Experimental-Physiologische Untersuchungen* (Darmstadt: E. Merck AG).
- Seibt, J., Dumoulin, M.C., Aton, S.J., Coleman, T., Watson, A., Naidoo, N., and Frank, M.G. (2012). Protein synthesis during sleep consolidates cortical plasticity in vivo. *Curr. Biol.* 22, 676–682.
- Seigneur, J., and Timofeev, I. (2011). Synaptic impairment induced by paroxysmal ionic conditions in neocortex. *Epilepsia* 52, 132–139.
- Siegel, J.M. (2005). Clues to the functions of mammalian sleep. *Nature* 437, 1264–1271.
- Sjöström, P.J., Rancz, E.A., Roth, A., and Häusser, M. (2008). Dendritic excitability and synaptic plasticity. *Physiol. Rev.* 88, 769–840.
- Steriade, M., and Timofeev, I. (2003). Neuronal plasticity in thalamocortical networks during sleep and waking oscillations. *Neuron* 37, 563–576.
- Steriade, M., Nuñez, A., and Amzica, F. (1993). A novel slow (< 1 Hz) oscillation of neocortical neurons *in vivo*: depolarizing and hyperpolarizing components. *J. Neurosci.* 13, 3252–3265.
- Steriade, M., Timofeev, I., and Grenier, F. (2001). Natural waking and sleep states: a view from inside neocortical neurons. *J. Neurophysiol.* 85, 1969–1985.
- Timofeev, I., Grenier, F., and Steriade, M. (2001). Disfacilitation and active inhibition in the neocortex during the natural sleep-wake cycle: an intracellular study. *Proc. Natl. Acad. Sci. USA* 98, 1924–1929.
- Tononi, G., and Cirelli, C. (2003). Sleep and synaptic homeostasis: a hypothesis. *Brain Res. Bull.* 62, 143–150.
- Tononi, G., and Cirelli, C. (2006). Sleep function and synaptic homeostasis. *Sleep Med. Rev.* 10, 49–62.
- Vyazovskiy, V.V., Cirelli, C., Pfister-Genskow, M., Faraguna, U., and Tononi, G. (2008). Molecular and electrophysiological evidence for net synaptic potentiation in wake and depression in sleep. *Nat. Neurosci.* 11, 200–208.
- Zamanillo, D., Sprengel, R., Hvalby, O., Jensen, V., Burnashev, N., Rozov, A., Kaiser, K.M., Köster, H.J., Borchardt, T., Worley, P., et al. (1999). Importance of AMPA receptors for hippocampal synaptic plasticity but not for spatial learning. *Science* 284, 1805–1811.